On the Promoting Role of Ag in Selective Hydrogenation Reactions over Pd−Ag Bimetallic Catalysts: A Theoretical Study

Silvia González,[†] Konstantin M. Neyman,*[,†,‡] Shamil Shaikhutdinov,[§] Hans-Joachim Freund,[§] and Francesc Illas[†]

Departament de Química Física i Centre especial de Recerca en Química Teòrica, Universitat de Barcelona i Parc Científic de Barcelona, 08028 Barcelona, Spain, Institució Catalana de Recerca i Estudis Avançats (ICREA), 08010 Barcelona, Spain, and Abteilung Chemische Physik, Fritz-Haber-Institut der Max-Planck-Gesellschaft, 14195 Berlin, Germany

Received: February 26, 2007

The surface structure of Pd−Ag alloy and its alteration in the presence of atomic hydrogen have been studied using density functional calculations on $Pd_{1-x}Ag_x(111)$ ($x \approx 0.2$) models. In the absence of an adsorbate, silver atoms are found to segregate on the surface, in line with previous experimental observations under vacuum conditions. At equilibrium, the surface is predicted to expose mainly Ag atoms. Isolated Pd atoms incorporated in this Ag-rich layer appear to be slightly preferred over the Pd_2 dimers. Increasing the coverage of adsorbed H atoms on the Pd−Ag substrate gradually suppresses surface segregation of silver, such that migration of all surface Ag atoms into the subsurface region becomes favorable at a H coverage of ∼0.25 ML. For the latter structures, with solely Pd atoms in the surface layer and Ag atoms in the subsurface layer, the propensity of H to be accommodated in interstitial sites below the surface layer essentially vanishes: subsurface H atoms are predicted to be energetically driven to escape to the surface without an activation barrier. These results might have strong implications in understanding the promoting role of Ag in selective hydrogenation reactions over Pd−Ag catalysts. The presented adsorbate-induced resegregation in bimetallic systems is a general concept applicable to a broad variety of catalytic systems and advanced materials.

1. Introduction

Bimetallic systems based on palladium with addition of silver are widely used as selective hydrogenation catalysts[1−3] and membranes for hydrogen separation.[4,5] Knowledge of the surface composition of $Pd_{1-x}Ag_x$ materials, particularly in the presence of hydrogen, is crucial for elucidating reaction mechanisms on these materials.

The composition of clean surfaces of disordered binary $Pd_{1-x}Ag_x$ alloys is known to differ significantly from that of the bulk, because of the strong surface segregation of silver. For instance, according to scanning tunneling microscopy (STM) studies of a $Pd_{0.67}Ag_{0.33}$ alloy single crystal annealed at 720 K, only ∼5% of atoms on the (111) surface are Pd.[6] In general, segregation of one component in bimetallic systems appears to be a very delicate phenomenon that depends on small variations in structure, stoichiometry, and external conditions, as has recently been shown for PdZn alloys.[7−9] Recent first-principles theoretical studies have also corroborated and rationalized the strong propensity of Ag,[10,11] similarly to the other coinage metals Cu and Au,[11] to segregate on the surface of binary alloys with Pd. Density functional (DF) calculations on the thermodynamics of the catalytic hydrogenation of acetylene−ethylene mixtures have been performed on simple models of Pd−Ag alloy surfaces, including Pd(111), $Pd_{0.75}Ag_{0.25}(111)$, $Pd_{0.5}Ag_{0.5}(111)$, and Ag(111), completely neglecting surface restructuring caused by adsorbates.[2]

However, the salient structural (and thus electronic) features of Pd−Ag surfaces can be significantly changed in the presence of adsorbates. For example, reverse (Pd) surface segregation (by ∼5% with respect to the bulk concentration) has been reported on the high-hydrogen-pressure side of $Pd_{75}Ag_{25}$ membranes as measured ex situ by X-ray photoelectron spectroscopy.[5] Merely on the basis that Pd−H binding is stronger than Ag−H binding, it has been suggested that hydrogen available under acetylene hydrogenation conditions affects the surface composition of Pd−Ag catalysts in favor of increasing surface concentration of Pd.[12] This, in turn, should be critical for the complex interplay between surface and subsurface hydrogen species, which are proposed to govern hydrogenation reactions on Pd and Pd−Ag model catalysts.[13,14]

Despite its immediate importance in terms of reactivity, the effect of hydrogen on the surface structure of Pd−Ag catalysts is not yet understood in detail at the microscopic level. The present DF study extends and deepens our knowledge of the surface structure of $Pd_{1-x}Ag_x$ materials, both clean and when interacting with H, and focuses on the promoting role of Ag in selective hydrogenation reactions over Pd−Ag catalysts. Moreover, we propose resegregation in bimetallic materials caused by the presence of reactants preferably interacting with one of the components as a concept that, to the best of our knowledge, has not yet been well documented in the literature. This concept is expected to be of general validity for various materials based on bi- and polymetallic systems.

The paper is organized as follows: Section 2 describes the computational method and models employed. In section 3, we first discuss the local composition and conceivable surface structures of clean $Pd_{0.8}Ag_{0.2}(111)$ slabs. We then address the

* To whom correspondence should be addressed. E-mail: konstantin.neyman@icrea.es.
† Universitat de Barcelona i Parc Científic de Barcelona.
‡ Institució Catalana de Recerca i Estudis Avançats (ICREA).
§ Fritz-Haber-Institut der Max-Planck-Gesellschaft.

10.1021/jp071584v CCC: $37.00
Published on Web 04/19/2007

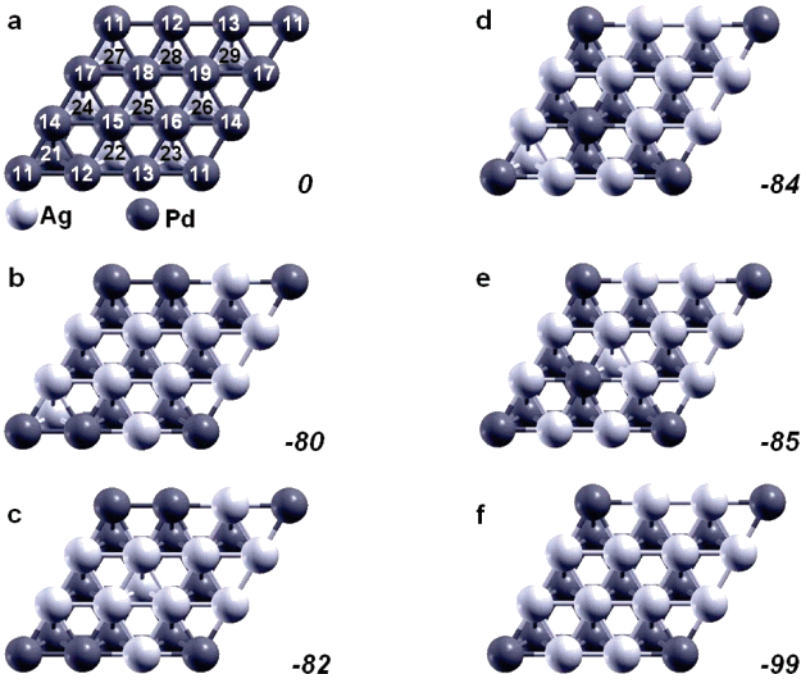

Figure 1. Top view of the upper two layers of a four-layer slab of $Pd_{28}Ag_8$ with the surface supercell (3×3), representing the (111) surface of $Pd_{1-x}Ag_x$ ($x \approx 0.2$) materials of different local stoichiometry. (The edge and corner atoms of the supercell that are shown count only as one-half and one-quarter atoms, respectively.) Models $Pd_{9-n}Ag_n/Pd_{1+n}Ag_{8-n}$ are denoted by the compositions of the surface/subsurface layers, with *n* being the number of Ag atoms in the surface layer: (a) $Pd_9/Pd_1(21)Ag_8$, (b) $Pd_2(11,12)Ag_7/Pd_8Ag_1(21)$, (c) $Pd_2(11,12)Ag_7/Pd_8Ag_1(25)$, (d) $Pd_2(11,15)Ag_7/Pd_8Ag_1(21)$, (e) $Pd_2(11,15)Ag_7/Pd_8Ag_1(25)$, (f) $Pd_1(11)Ag_8/Pd_9$. In parentheses are the positions of the minority-type atoms in each of the layers, according to the labels in the upper panel. Atomic spheres: light gray, Ag; dark gray, Pd. Also shown are total energy differences (italics, in kJ mol^{-1}) with respect to the least stable structure Pd_9/Pd_1Ag_8 (a).

structural changes in $Pd_{0.8}Ag_{0.2}$ induced by its interaction with atomic hydrogen in which one of the central issues is determining the propensity for subsurface hydrogen species to stabilize. Finally, in section 4, we summarize our results.

2. Computational Details and Models

DF calculations were performed with the Vienna ab initio simulation package (VASP).[15−17] The Kohn−Sham one-electron wave functions were expanded in a basis of plane waves with cutoff value of 340 eV for the kinetic energy. The interaction between atomic cores and valence electrons was described by the projector augmented wave (PAW) method.[18,19] The blocked Davidson approach was employed as the electronic minimization algorithm. The Gaussian scheme with the smearing value of $k_BT = 0.2$ eV was used to determine the occupancies at the spin-restricted level; upon convergence of the electron density for each single-point geometry, the total energy was extrapolated to $k_BT = 0$ eV. For integration over the Brillouin zone of the surface unit cell, we utilized a $5 \times 5 \times 1$ Monkhorst−Pack grid of *k* points.[20]

The $Pd_{1-x}Ag_x(111)$ surface was modeled as slabs containing four atomic layers. A 3×3 supercell with nine Pd + Ag atoms per atomic layer was chosen, allowing for the study of adsorbate coverages as low as $^1/_9$ ML. The vacuum spacing of ~1.2 nm was introduced to separate the periodically repeated slabs. The positions of the metal atoms in the two uppermost layers and, when applicable, of the H atoms were optimized using a conjugate gradient algorithm; two substrate layers at the bottom of each slab were kept fixed at the experimental geometry corresponding to bulk Pd characterized by nearest Pd−Pd distances of 275 pm.[21] The adsorbed/interstitial H atoms were placed on one side of the metal slabs. All Cartesian coordinates of atoms included in the variation were optimized until the force acting on each atom was ≤0.4 eV/nm.

The local density approximation (LDA, VWN parametrization[22]) was utilized to optimize the structure. This approach yields accurate geometric (and vibrational spectroscopy) parameters, whereas generalized-gradient approximation (GGA) improves binding energies[23,24] but often overestimates experimental interatomic distances, especially for such heavy elements as Pd.[25] Thus, energies presented in the following were calculated for LDA-optimized geometries using GGA exchange-correlation functional PW91[26] in a single-point manner. Differences of ~2 pm in distances and ~5 kJ mol^{-1} in relative energies calculated using this approach are estimated to be meaningful.

We considered the bimetallic substrate $Pd_{1-x}Ag_x$ with a Ag content of $x \approx 0.2$. To facilitate comparison between the various substrate models under scrutiny, the supercell of each model consisted of 28 Pd and 8 Ag atoms, $Pd_{28}Ag_8$. Two limiting situations were studied: (i) complete absence of silver segregation, with the surface layer (L1) composed solely of Pd atoms and the 8 Ag atoms of the unit cell located in the subsurface layer (L2), Pd_9/Pd_1Ag_8 (Figure 1a), and (ii) complete silver segregation, with all Ag atoms in the surface layer, Pd_1Ag_8/Pd_9 (Figure 1f). Four models of the intermediate L1/L2 stoichiometry Pd_2Ag_7/Pd_8Ag_1 (Figure 1b−e) were also studied, as well as the reference system Pd_9/Pd_9 with all L1/L2 atoms being Pd while the 8 Ag atoms were in the bottom layer (L4) of the slab, most distant from the adsorbed H.

Only phenomena occurring on the ordered $Pd_{1-x}Ag_x(111)$ surfaces are addressed directly. Nevertheless, as is documented in the following sections, adsorption (and reactivity) phenomena on the bimetallic materials under scrutiny are governed by ensemble effects. Thus, qualitative results of this study are expected to be applicable to surfaces of less ordered Pd−Ag samples, especially when the latter expose surface sites similar to those considered for the $Pd_{1-x}Ag_x(111)$ models.

3. Surface Structure of $Pd_{0.8}Ag_{0.2}(111)$

3.1. Clean Substrate. The relative energies of several conceivable structural arrangements of clean slabs formed by the supercell $Pd_{28}Ag_8$ are listed in Figure 1. One should note that, according to our topological analysis of the charge density,[27] neither Pd nor Ag atoms acquire noticeable charge in Pd−Ag systems: surrounding a Pd atom with Ag atoms results in minor (if any) electron depletion of the former, limited to ∼0.05 *e*. Thus, a significant negative binding energy shift of −0.7 eV, measured by X-ray photoelectron spectroscopy for Ag 3d core level in Pd−Ag alloys as compared to pure Ag,[13,28,29] should probably be assigned to effects other than Pd−Ag charge transfer.[30]

The least stable (at 0 K) model under scrutiny was found to be that with no Ag atoms in the topmost surface layer, Pd_9/Pd_1Ag_8 (Figure 1a). Displacement of all eight Ag atoms from the subsurface layer to the surface layer, resulting in the model Pd_1Ag_8/Pd_9 (Figure 1f), is accompanied by stabilization of ∼100 kJ mol^{-1} (∼12 kJ mol^{-1} per Ag atom). Intermediate models with seven surface and one subsurface Ag atoms, Pd_2Ag_7/Pd_8Ag_1 (Figure 1b−e), are destabilized with respect to Pd_1Ag_8/Pd_9 by 14−19 kJ mol^{-1}. This is similar to findings from previous theoretical[10,11,31] and experimental[6] studies on different alloy compositions, and the propensity of the silver component to segregate on the surface of $Pd_{0.8}Ag_{0.2}$ material is therefore evident. However, as mentioned previously, the thermodynamic driving force for the segregation of Ag in Pd is rather modest,[31] which makes the efficient counteracting of the segregation under certain reaction conditions likely (see below).

No detailed theoretical information on the microscopic picture of the structure and distribution of surface sites exposed by Pd−Ag is available in the literature. In STM studies of $Pd_{0.67}Ag_{0.33}$, no indication of the presence of a second metal component (Pd) was found at the equilibrated (100) surface.[6] The equilibration of $Pd_{0.67}Ag_{0.33}(111)$ crystals at 820 K resulted in a surface composition of only ∼5% Pd, and an overwhelming majority of palladium atoms on the surface formed isolated sites, i.e., were entirely surrounded by silver atoms.[6] There, the trend to build single surface Pd sites was enhanced, and that to build double sites (two nearest Pd atoms) was reduced compared to what is expected from a random distribution of surface atoms; almost no sites with three nearest Pd neighbors (triple, Pd_3) were identified.[6] Our calculated results (Figure 1b−e) corroborate these[6] and other similar[13,32] experimental findings. Indeed, among the Pd_2Ag_7/Pd_8Ag_1 models studied, those with two single Pd atoms, Pd(11) and Pd(15), in the surface layer of $Pd_{0.8}Ag_{0.2}$-(111) (Figure 1d,e) were found to be 2−5 kJ mol^{-1} more stable than the congeners exposing one Pd_2 pair, Pd(11)−Pd(12) (Figure 1b,c). However, the preference for Pd_1 sites over Pd_2 sites appears to be small enough to suggest that the overall energetic balance can be qualitatively affected by modifying external conditions or by going from flat (111) terraces to surface irregularities, which are abundant on the surfaces of bimetallic nanoparticles.[13] Thus, the presence of Pd_2 sites on the Pd−Ag surface should not be completely neglected when interpreting experimental data, in contrast to the much rarer surface Pd_3 ensembles.

All $Pd_{0.8}Ag_{0.2}(111)$ models under study showed that the surface Ag atoms are located higher than the surrounding Pd atoms, by ∼10 pm on average. This agrees with a simple consideration of the atomic radii of the metals, as that of Ag is larger than that of Pd (144.5 vs 137.6 pm). The fact that STM studies[6] revealed isolated Pd atoms on the $Pd_{0.67}Ag_{0.33}(111)$ surface that are ∼25 pm higher than the Ag atoms must therefore be assigned to electronic effects of STM imaging.

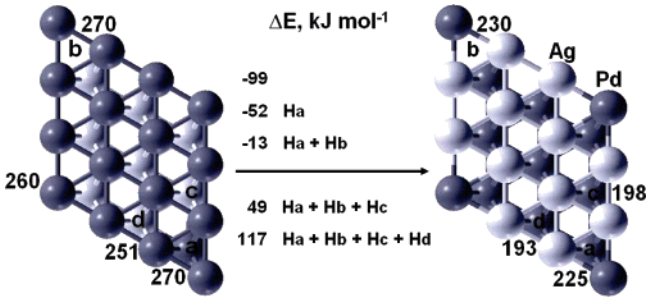

Figure 2. Sketches of the upper two layers of $Pd_{28}Ag_8$ substrate slab models, in which all Ag atoms (gray spheres) are located either in the subsurface layer, Pd_9/Pd_1Ag_8 (left panel), or in the surface layer, Pd_1Ag_8/Pd_9 (right panel). Four 3-fold-hollow positions of adsorbed atoms H are labeled a−d, and the calculated adsorption energies of atomic H on these sites (in kJ mol^{-1}, eventually in the presence of other coadsorbed H atoms) are shown. Also shown are total energy differences (in kJ mol^{-1}; negative signs indicate stabilization in the direction of the arrow) between the adsorption complexes with the same number of H atoms on these two substrate models.

3.2. Interactions with Hydrogen. Atomic H is known to be present on Pd−Ag catalysts under hydrogenation reaction conditions. At low coverage, on clean (111) surfaces of both Pd(111) and Ag(111), atomic H is preferentially adsorbed on 3-fold-hollow sites, but the interaction (DF PW91 data) with Pd(111), ∼270 kJ mol^{-1},[33] is notably stronger than that with Ag(111), ∼200 kJ mol^{-1}.[34] This energy difference of 70 kJ mol^{-1} is comparable to the energy release accompanying the segregation of silver on the surface of Pd−Ag alloys (see Figure 1). Furthermore, it implies that, on bimetallic $Pd_{1-x}Ag_x$ surfaces, atomic H more favorably interacts with those sites that are formed by as many Pd atoms as possible and avoids sites mainly built of Ag atoms. Therefore, significant surface restructuring of $Pd_{1-x}Ag_x$ materials should be expected to accompany increased coverage of adsorbed H.

Our results, presented in Figure 2, corroborate this assumption and quantify some details of such hydrogen-induced restructuring. We chose two models of $Pd_{0.8}Ag_{0.2}(111)$ substrate that were considered in the previous section: the least stable system with no Ag atoms in the surface layer, Pd_9/Pd_1Ag_8, and the most stable system, Pd_1Ag_8/Pd_9, in which all eight Ag atoms are on the surface. We increased the hydrogen coverage (θ_H) on each of these two models by subsequent occupation by H of the following hollow adsorption sites (see Figure 2): a ($\theta_H = {}^1/_9$ ML), a + b ($\theta_H = {}^2/_9$ ML), a + b + c ($\theta_H = {}^1/_3$ ML), and a + b + c + d ($\theta_H = {}^4/_9$ ML). Then, for each θ_H value, we compared the total energies of the adsorption systems on the Pd_9/Pd_1Ag_8 and Pd_1Ag_8/Pd_9 slab models (left and right panels of Figure 2, respectively); the energy differences ("reaction energies", in kJ mol^{-1}) are shown at the arrow connecting the two panels.

These results deserve a closer look. The first issue is how the adsorption energy values of H on the bimetallic substrate compare to those on clean Pd(111) and Ag(111). When the upper layer of the most stable 3-fold-hollow adsorption sites of $Pd_{0.8}Ag_{0.2}(111)$ is completely built of Pd atoms, Pd_3 sites, the calculated adsorption energy of H, 270 kJ mol^{-1} (Figure 2, left panel, sites a and b), remains essentially the same as on clean Pd(111).[33] Increasing the coverage of H further (Figure 2, left panel, sites c and d) reduces the adsorption energy on Pd_3 sites very slightly, by only 10 and 19 kJ mol^{-1}, respectively. This is a nice illustration of a more general observation in which the so-called ensemble effect[35,36] basically defines properties of

bimetallic surfaces; in other words, only the structure and composition of the nearest part of adsorption sites are crucial for interaction with these sites.[8,33,37−39] Switching to the right panel of Figure 2, one finds that the calculated adsorption energies of H with the sites that include one surface Pd atom, $PdAg_2$ (sites a and b), 225 and 230 kJ mol^{-1}, are almost equal to each other and intermediate between the values on Pd(111) and Ag(111). However, when H is adsorbed on sites that expose a Ag_3 surface fragment, the adsorption energy becomes very close to that on clean Ag(111),[34] 198 kJ mol^{-1} (site c), or just slightly smaller, 193 kJ mol^{-1} (site d), which is partly due to lateral H−H interactions. Thus, the ensemble effect is again the decisive factor for rationalizing the calculated data.

The next question is how adsorbed hydrogen atoms affect the relative stabilities of various surface structures of the Pd−Ag substrate. We saw in the previous subsection that, in the case of the clean $Pd_{0.8}Ag_{0.2}$(111) surface, the model with Ag atoms located in the topmost layer, Pd_1Ag_8/Pd_9, is stabilized by 99 kJ mol^{-1} compared to the "unsegregated" model Pd_9/Pd_1Ag_8. When adsorption site a on each of these two slab models is occupied by a H atom, the overall energy preference of $H_a/Pd_1Ag_8/Pd_9$ over $H_a/Pd_9/Pd_1Ag_8$ decreases to 52 kJ mol^{-1} (Figure 2). Adsorption of one more atom, now on b sites, makes the $(H_a + H_b)/Pd_1Ag_8/Pd_9$ system just 13 kJ mol^{-1} more stable than $(H_a + H_b)/Pd_9/Pd_1Ag_8$. A further increase of H coverage, modeled by the occupation of c sites, results in the reverse stability: adsorption system $(H_a + H_b + H_c)/Pd_9/Pd_1Ag_8$ with Ag atoms in the subsurface layer of the bimetallic substrate becomes 49 kJ mol^{-1} more stable than the "segregated" $(H_a + H_b + H_c)/Pd_1Ag_8/Pd_9$ system (Figure 2). This trend of relative stabilization of the Pd_9/Pd_1Ag_8 slab over Pd_1Ag_8/Pd_9, because of the greater amounts of adsorbed H, is continued for the systems with $H_a + H_b + H_c + H_d$ adsorbates. From this series of relative energies, one can conclude that adsorbed hydrogen definitely favors stabilization of Pd−Ag structures with Pd-rich surfaces and Ag-rich cores, which is proposed to be advantageous for catalytic performance.[12] Indeed, such a low hydrogen coverage as $\sim 1/4$ ML already appears to be sufficient to counteract the thermodynamic driving force for the segregation of Ag on the $Pd_{0.8}Ag_{0.2}$(111) surface. It is also worth emphasizing that the energetic balance just discussed is essentially quantitatively rationalized in terms of the adsorption energies of hydrogen (and the differences between them) on various sites as defined by the exposed surface ensembles. The predicted surface segregation of Pd in the H_2 atmosphere seems to be rapid under real reaction conditions ($\sim$350 K), as the activation barrier for the Pd−Ag place exchange is rather low, $\leq$50 kJ mol^{-1}.[40]

The last issue to be addressed in this article is the propensity of Pd−Ag structures to stabilize subsurface atomic H. This is important in light of the observation that the complete (and undesirable) hydrogenation of acetylene to ethane on Pd−Ag catalysts is enhanced in the presence of subsurface hydrogen.[12] Thus, to suppress full hydrogenation and increase selectivity to ethylene, formation of subsurface H needs to be hindered. We examined whether Pd−Ag materials with Pd-rich surfaces and Ag-rich cores, corresponding to the Pd_9/Pd_1Ag_8 model that is stabilized by moderate coverage of adsorbed H (vide supra), suppress the formation of subsurface H.

Our results for surface/subsurface migration of H calculated for the three models Pd_1Ag_8/Pd_9, Pd_9/Pd_9, and Pd_9/Pd_1Ag_8 at the coverage $\theta_H = 1/9$ ML are presented in Table 1. We first consider the Pd_1Ag_8/Pd_9 model, representative of a clean segregated $Pd_{0.8}Ag_{0.2}$(111) surface, at low H coverage. The fcc-

TABLE 1: Calculated Distances and Relative Energies Characterizing H Atoms Adsorbed on fcc or hcp Sites of Four-Layer Slabs of $Pd_{28}Ag_8$ with Various Compositions of the Layers or in Interstitial oss or tss Sites between the Surface/Subsurface Layers L1/L2[a]

position of H[b]	H−Pd(L1)/ H−Pd(L2) (pm)	H−Ag (pm)	Δz_{L1} (H) (pm)	Δz_{L2} (H) (pm)	$\Delta E_{surf\rightarrow subs}$ (kJ mol^{-1})
L1/L2 = Pd_1Ag_8/Pd_9					
fcc(Ag_3/Pd_3)		187	98		
oss(Ag_3/Pd_3)	175	236	−167	60	−17
fcc(Pd_1Ag_2/Pd_3)	168	197	94		
oss(Pd_1Ag_2/Pd_3)	189/179	227	−133	87	15
hcp(Ag_3/Pd_1)		188	100		
tss(Ag_3/Pd_1)	166	182	−74	166	24
hcp(Pd_1Ag_2/Pd_1)	168	200	96		
tss(Pd_1Ag_2/Pd_1)	167/169	187	−63	169	40
L1/L2 = Pd_9/Pd_9					
fcc(Pd_3/Pd_3)	180		80		
oss(Pd_3/Pd_3)	182/217		−80	146	35
hcp(Pd_3/Pd_1)	180		79		
tss(Pd_3/Pd_1)	174/188		−38	188	27
L1/L2 = Pd_9/Pd_1Ag_8					
hcp(Pd_3/Pd_1)	179		78		
tss(Pd_3/Pd_1)	176/183		−45	176	27
fcc(Pd_3/Ag_3)	178		73		
oss(Pd_3/Ag_3)[c]	–		–		–
hcp(Pd_3/Ag_1)	179		75		–
tss(Pd_3/Ag_1)[c]	–		–		

[a] H−X(Ln), where X is the nearest Pd/Ag atom of layer Ln = 1, 2, average interatomic distance; Δz_{Ln}(H), height of H over (positive sign) or under (negative sign) the average vertical position of substrate atoms in the layer Ln; $\Delta E_{surf\rightarrow subs}$, migration energy of a single H atom from a position on the surface down into the corresponding subsurface position (positive sign implies endothermic process). $\theta_H = 1/9$ ML. [b] Defined as the position of H in the starting geometry for optimization. Such notations as fcc(Pd_1Ag_2/Pd_3) and oss(Pd_1Ag_2/Pd_3) mean that the fcc adsorption site and octahedral subsurface (oss) site, respectively, are formed of one Pd and two Ag atoms in the surface layer and three Pd atoms in the subsurface layer. [c] Unstable; optimization of the subsurface structure resulted in spontaneous displacement of H to the adsorption position on the surface without activation barrier.

(Ag_3/Pd_3) adsorption site exposing surface ensemble Ag_3 is energetically destabilized by 17 kJ mol^{-1} when accommodating one H atom per supercell, compared to the case when the H atom is located in the octahedral subsurface (oss) hole lying below. Thus, H can be stored in the subsurface in the oss(Ag_3/Pd_3) interstitial positions. However, if just one of these three surface Ag atoms is substituted by Pd, migration of the H atom from fcc(Pd_1Ag_2/Pd_3) to oss(Pd_1Ag_2/Pd_3) sites becomes unfavorable by 15 kJ mol^{-1}. This value should be compared to the 35 kJ mol^{-1} (Table 1) calculated for fcc → oss displacement of H in Pd_3/Pd_3 sites, which was modeled by a Pd_9/Pd_9 slab with all Ag atoms in the bottom layer; DF calculations for a Pd_{79} nanocluster give 50 kJ mol^{-1}.[41] Therefore, the thermodynamic driving force for H to migrate into oss sites on Ag-rich Pd−Ag surfaces seems to be even stronger than that on pure Pd. As for the hcp → tss (tetrahedral subsurface site) migration channel, our results for the Ag-rich model of the Pd−Ag surface are quantitatively similar to those for the model of pure Pd.

What happens with the accommodation of the H subsurface in the case of Pd-rich Pd−Ag surfaces, which we propose to be representative at $\theta_H > 1/4$ ML (0 K), appears to be even more interesting. The H(hcp) → H(tss) structural parameters and energetic balance for the Pd_3/Pd_1 sites of the Pd_9/Pd_1Ag_8 model are computed to be very close to the corresponding values for these sites on pure Pd (Pd_9/Pd_9 model). However, the number of these sites in the Pd_9/Pd_1Ag_8 model is low, and it remains to be examined whether the increase of H coverage on Pd-rich

Pd−Ag surfaces can make the occupation of the subsurface tss-(Pd_3/Pd_1) positions favorable. The most abundant sites in the Pd_9/Pd_1Ag_8 model are the Pd_3/Ag_3 and Pd_3/Ag_1 surface sites. During optimization of the position of the H atom, which is initially located in each of these interstitial sites, the H atom gradually moved toward the surface, so that the resulting geometries corresponded to H adsorption on the fcc(Pd_3/Ag_3) and hcp(Pd_3/Ag_1) sites, respectively, instead of the oss and tss structures. This means, that hydrogen *spontaneously* leaves subsurface sites formed by surface Pd and subsurface Ag atoms; the nonactivated character of this migration to the surface was confirmed by our calculations. Thus, we demonstrate that the apparently favorable surface restructuring of Pd−Ag catalysts for hydrocarbon hydrogenation, caused by hydrogen adsorption, also leads to considerably hindered formation of subsurface hydrogen. This effect is proposed to be advantageous for improving the selectivity of these catalysts.

4. Summary and Conclusions

The surface segregation of silver on clean $Pd_{0.8}Ag_{0.2}(111)$ was shown to lead to a noticeable energy gain: relocation of one silver atom from the subsurface layer of $Pd_{0.8}Ag_{0.2}(111)$ to the surface releases ~15 kJ mol^{-1} in the 3×3 surface cell. Thus, such a material under vacuum conditions is expected to be almost completely covered by a layer of Ag atoms, in line with previous experimental and theoretical findings. Among the Pd atoms still present in the surface layer, single Pd_1 centers are slightly preferred over Pd_2 dimers.

Adsorbed atomic H was found to dramatically reduce the propensity of silver to segregate on the surface. Increasing the H coverage from $^1/_9$ ML to $^4/_9$ ML gradually diminishes the energy gain due to Ag segregation. As a result, reverse segregation starts to take place when the H coverage is greater than $^1/_4$ ML, whereby the surface layer is formed mainly of Pd atoms.

At low H coverages ($^1/_9$ ML), we quantified the energy of subsurface diffusion of hydrogen depending on the composition of surface/subsurface sites on the $Pd_{0.8}Ag_{0.2}(111)$ models. On the surface with segregated Ag atoms, displacement of adsorbed H from fcc(Ag_3/Pd_3) sites into the corresponding interstitial subsurface position is energetically favored, indicating a high probability that subsurface H can be stabilized. In contrast, when the surface layer is formed solely of Pd atoms and all Ag atoms are located in the subsurface layer, the interstitial H atoms are predicted to escape from both oss(Pd_3/Ag_3) and tss(Pd_3/Ag_1) sites to the surface *spontaneously*, without an activation barrier.

Our results fully support the hypothesis that Ag atoms, mostly located in the subsurface region under hydrogen-rich conditions, suppress the formation of subsurface hydrogen and, hence, the full hydrogenation pathway in reactions with unsaturated hydrocarbons. The results also highlight the importance of ambient-induced segregation phenomena for rationalizing the promoting effects of additives to hydrogenation metal catalysts. The discussed concept of surface resegregation caused by ambient gas adsorbates having a higher affinity to one of the components in bimetallic materials is expected to be of general importance and applicable across a broad range of surface processes on various substrates, well beyond hydrogenation reactions on $Pd_{1-x}Ag_x$ catalysts.

Acknowledgment. S.G. is grateful to the Universitat de Barcelona for a predoctoral fellowship. This work was supported by the Spanish Ministry of Education and Science (Grants CTQ2005-08459-CO2-01 and UNBA05-33-001) and the Generalitat de Catalunya (2005SGR00697, 2005 PEIR 0051/69, and Distinció per a la Promoció de la Recerca Universitària granted to F.I.). A significant part of the calculations was carried out on the Marenostrum supercomputer through a grant from the Barcelona Supercomputer Center.

References and Notes

(1) Jin, Y.; Datye, A. K.; Rightor, E.; Gulotty, R.; Waterman, W.; Smith, M.; Holbrook, M.; Maj, J.; Blackson, J. *J. Catal*. **2001**, *203*, 292.

(2) Sheth, P. A.; Neurock, M.; Smith, C. M. *J. Phys. Chem. B* **2005**, *109*, 12449.

(3) Zea, H.; Lester, K.; Datye, A. K.; Rightor, E.; Gulotty, R.; Waterman, W.; Smith, M. *Appl. Catal. A* **2005**, *282*, 237.

(4) Shu, J.; Grandjean, B. P. A.; Vanneste, A.; Kaliaguine, S. *Can. J. Chem. Eng.* **1991**, *69*, 1036.

(5) Shu, J.; Bongondo, B. E. W.; Grandjean, B. P. A.; Adnot, A.; Kaliaguine, S. *Surf. Sci*. **1993**, *291*, 129.

(6) Wouda, P. T.; Schmid, M.; Nieuwenhuys, B. E.; Varga, P. *Surf. Sci*. **1998**, *417*, 292.

(7) Chen, Z.-X.; Neyman, K. M.; Rösch, N. *Surf. Sci*. **2004**, *548*, 291.

(8) Neyman, K. M.; Sahnoun, R.; Inntam, C.; Hengrasmee, S.; Rösch, N. *J. Phys. Chem. B* **2004**, *108*, 5424.

(9) Bayer, A.; Flechtner, K.; Denecke, R.; Steinrück, H.-P.; Neyman, K. M.; Rösch, N. *Surf. Sci.* **2006**, *600*, 78.

(10) Ropo, M.; Kokko, K.; Vitos, L.; Kollár, J. *Phys. Rev. B* **2005**, *71*, 045411.

(11) Løvvik, O. M. *Surf. Sci*. **2005**, *583*, 100.

(12) Khan, N. A.; Shaikhutdinov, S.; Freund, H.-J. *Catal. Lett*. **2006**, *108*, 159.

(13) Doyle, A. M.; Shaikhutdinov, S. K.; Jackson, S. D.; Freund, H.-J. *Angew. Chem., Int. Ed.* **2003**, *42*, 5240.

(14) Khan, N. A.; Uhl, A.; Shaikhutdinov, S.; Freund, H.-J. *Surf. Sci*. **2006**, *600*, 1849.

(15) Kresse, G.; Furthmüller, J. *Phys. Rev. B* **1996**, *54*, 11169.

(16) Kresse, G.; Hafner, J. *Phys. Rev. B* **1993**, *47*, 558.

(17) Kresse, G.; Furthmüller, J. *Comput. Mater. Sci*. **1999**, *6*, 15.

(18) Blöchl, P. E. *Phys. Rev. B* **1994**, *50*, 17953.

(19) Kresse, G.; Joubert, D. *Phys. Rev. B* **1999**, *59*, 1758.

(20) Monkhorst, H. J.; Pack, J. D. *Phys. Rev. B* **1976**, *13*, 5188.

(21) *CRC Handbook of Chemistry and Physics*, 77th ed.; Lide, D. R., Ed.; CRC Press: Boca Raton, FL, 1996.

(22) Vosko, S. H.; Wilk, L.; Nusair, M. *Can. J. Phys.* **1980**, *58*, 1200.

(23) Ziegler, T. *Chem. Rev.* **1991**, *91*, 651.

(24) Görling, A.; Trickey, S. B.; Gisdakis, P.; Rösch, N. In *Topics in Organometallic Chemistry*; Brown, J., Hofmann, P., Eds.; Springer: Heidelberg, Germany, 1999; Vol. 4, p 109.

(25) Krüger, S.; Vent, S.; Nörtemann, F.; Staufer M.; Rösch, N. J. *Chem. Phys.* **2001**, *115*, 2082.

(26) Perdew, J. P.; Wang, Y. *Phys. Rev. B* **1992**, *45*, 13244.

(27) Henkelman, G.; Arnaldsson, A.; Jónsson, H. *Comput. Mater. Sci*. **2006**, *36*, 354.

(28) Pervan, P.; Milun, M. *Surf. Sci.* **1992**, *264*, 135.

(29) Olovsson, W.; Bech, L.; Andersen, T. H.; Li, Z.; Hoffmann, S. V.; Johansson, B.; Abrikosov, I. A.; Onsgaard, J. *Phys. Rev. B* **2005**, *72*, 075444.

(30) Bagus, P. S.; Illas, F.; Pacchioni, G.; Parmigiani, F. *J. Electron Spectrosc. Relat. Phenom.* **1999**, *100*, 215.

(31) Ruban, A. V.; Skriver, H. L.; Nørskov, J. K. *Phys. Rev. B* **1999**, *59*, 15990.

(32) Nordermeer, A.; Kok, G. A.; Nieuwenhuys, B. E. *Surf. Sci*. **1986**, *165*, 375.

(33) Chen, Z.-X.; Neyman, K. M.; Lim, K. H.; Rösch, N. *Langmuir* **2004**, *20*, 8068.

(34) Mohammad, A. B.; Lim, K. H.; Yudanov, I. V.; Neyman, K. M.; Rösch, N. *Phys. Chem. Chem. Phys*. **2007**, *9*, 1247.

(35) Rodriguez, J. A. *Surf. Sci. Rep.* **1996**, *24*, 223.

(36) Ponec, V. *Appl. Catal. A: Gen.* **2001**, *222*, 31.

(37) González, S.; Sousa, C.; Illas, F. *J. Catal*. **2006**, *239*, 431.

(38) González, S.; Sousa, C.; Illas, F. *J. Phys. Chem. B* **2005**, *109*, 4654.

(39) González, S.; Sousa, C.; Illas, F. *Surf. Sci*. **2003**, *531*, 39.

(40) Baletto, F.; Mottet, C.; Ferrando, R. *Phys. Rev. B* **2002**, *66*, 155420.

(41) Yudanov, I. V.; Neyman, K. M.; Rösch, N. *Phys. Chem. Chem. Phys.* **2004**, *6*, 116.